J|A|C|S
ARTICLES

Distinct and Long-Lived Activity States of Single Enzyme Molecules

David M. Rissin,† Hans H. Gorris, and David R. Walt*

Department of Chemistry, Tufts University, Medford, Massachusetts 02155

Received January 4, 2008; E-mail: david.walt@tufts.edu

Abstract: Individual enzyme molecules have been observed to possess discrete and different turnover rates due to the presence of long-lived activity states. These stable activity states are thought to result from different molecular conformations or post-translational modifications. The distributions in kinetic activity observed in previous studies were obtained from small numbers of single enzyme molecules. Due to this limitation, it has not been possible to fully characterize the different kinetic and equilibrium binding parameters of single enzyme molecules. In this paper, we analyze hundreds of single β-galactosidase molecules simultaneously; using a high-density array of 50 000 fL-reaction chambers, we confirm the presence of long-lived kinetic states within a population of enzyme molecules. Our analysis has isolated the source of kinetic variability to k_{cat}. The results explain the kinetic variability within enzyme molecule populations and offer a deeper understanding of the unique properties of single enzyme molecules. Gaining a more fundamental understanding of how individual enzyme molecules work within a population should provide insight into how they affect downstream biochemical processes. If the results reported here can be generalized to other enzymes, then the stochastic nature of individual enzyme molecule kinetics should have a substantial impact on the overall metabolic activity within a cell.

Introduction

While enzymatic reactions conventionally have been studied on a macroscopic scale, the emergence of technologies capable of independently analyzing small reaction volumes has extended enzymatic analysis to the single molecule level.[1–15] Recent studies have measured broad distributions and dynamic fluctuations in the activity of single enzyme molecules that cannot be resolved in ensemble experiments.[16–25] Most research has focused on analyzing the turnover trajectories of individual enzyme molecules to detect reaction rate changes in sequential catalytic cycles, termed "dynamic disorder". Individual enzyme molecules have also been found to exhibit static heterogeneity, possessing unique and steady rate constants over long time periods.[1–4] In typical single molecule experiments that analyze static heterogeneity, there are an insufficient number of molecules analyzed to allow for comparison with bulk enzyme kinetics. In this paper, we describe a method that solves this shortcoming: each experiment interrogates hundreds of individual enzyme molecules, exposing highly distributed static

† Present address: Quanterix Corporation, 1 Kendall Square, Bldg. 1400, Cambridge, Massachusetts 02139.

(1) Craig, D. B.; Arriaga, E. A.; Wong, J. C. Y.; Lu, H.; Dovichi, N. J. *J. Am. Chem. Soc.* **1996**, *118*, 5245–5253.
(2) Craig, D. B.; Dovichi, N. J. *Can. J. Chem.* **1998**, *76*, 623–626.
(3) Xue, Q. F.; Yeung, E. S. *Nature* **1995**, *373*, 681–683.
(4) Craig, D. B.; Nachtigall, J. T.; Ash, H. L.; Shoemaker, G. K.; Dyck, A. C.; Wawrykow, T. M. J.; Gudbjartson, H. L. *J. Protein Chem.* **2003**, *22*, 555–561.
(5) Chiu, D. T.; Wilson, C. F.; Ryttsen, F.; Stromberg, A.; Farre, C.; Karlsson, A.; Nordholm, S.; Gaggar, A.; Modi, B. P.; Moscho, A.; Garza-Lopez, R. A.; Orwar, O.; Zare, R. N. *Science* **1999**, *283*, 1892–1895.
(6) Foquet, M.; Korlach, J.; Zipfel, W. R.; Webb, W. W.; Craighead, H. G. *Anal. Chem.* **2004**, *76*, 1618–1626.
(7) Gosalia, D. N.; Diamond, S. L. *Proc. Natl. Acad. Sci. U.S.A.* **2003**, *100*, 8721–8726.
(8) Gratzl, M.; Lu, H.; Matsimoto, T.; Yi, C.; Bright, G. R. *Anal. Chem.* **1999**, *71*, 2751–2756.
(9) Lipman, A. E.; Shuler, B.; Bakajin, O.; Eaton, W. A. *Science* **2003**, *301*, 1233–1235.
(10) Nagai, H.; Murakami, Y.; Yokoyama, K.; Tamiya, E. *Biosens. Bioelectron.* **2001**, *16*, 1015–1019.
(11) Nakano, M.; Komatsu, J.; Matsuura, S.; Takashima, K.; Katsura, S.; Mizuno, A. *J. Biotechnol.* **2003**, *102*, 117–124.
(12) Rondelez, Y.; Tresset, G.; Tabata, K. V.; Arata, H.; Fujita, H.; Takeuchi, S.; Noji, H. *Nat. Biotechnol.* **2005**, *23*, 361–365.
(13) Stamou, D.; Duschl, C.; Delamarche, E.; Vogel, H. *Angew. Chem., Int. Ed.* **2003**, *42*, 5580–5583.
(14) Whitesides, G. M. *Nat. Biotechnol.* **2003**, *21*, 1161–1165.
(15) Rotman, B. *Proc. Natl. Acad. Sci. U.S.A.* **1961**, *47*, 1981–91.
(16) English, B. P.; Min, W.; van Oijen, A. M.; Lee, K. T.; Luo, G.; Sun, H.; Cherayil, B. J.; Kou, S. C.; Xie, X. S. *Nat. Chem. Biol.* **2006**, *2*, 87–94.
(17) Flomenbom, O.; Velonia, K.; Loos, D.; Masuo, S.; Cotlet, M.; Engelborghs, Y.; Hofkens, J.; Rowan, A. E.; Nolte, R. J. M.; Van der Auweraer, M.; de Schryver, F. C.; Klafter, J. *Proc. Natl. Acad. Sci. U.S.A.* **2005**, *102*, 2368–2372.
(18) Lu, H. P.; Xun, L. Y.; Xie, X. S. *Science* **1998**, *282*, 1877–1882.
(19) van Oijen, A. M.; Blainey, P. C.; Crampton, D. J.; Richardson, C. C.; Ellenberger, T.; Xie, X. S. *Science* **2003**, *301*, 1235–1239.
(20) Velonia, K.; Flomenbom, O.; Loos, D.; Masuo, S.; Cotlet, M.; Engelborghs, Y.; Hofkens, J.; Rowan, A. E.; Klafter, J.; Nolte, R. J. M.; de Schryver, F. C. *Angew. Chem., Int. Ed.* **2005**, *44*, 560564, S560/1−S560/3.
(21) Zhuang, X.; Kim, H.; Pereira, M. J. B.; Babcock, H. P.; Walter, N. G.; Chu, S. *Science* **2002**, *296*, 1473–1476.
(22) Min, W.; Luo, G.; Cherayil, B. J.; Kou, S. C.; Xie, X. S. *Phys. Rev. Lett.* **2005**, *94*, 198302/1–198302/4.
(23) Yang, H.; Luo, G.; Karnchanaphanurach, P.; Louie, T.-M.; Rech, I.; Cova, S.; Xun, L.; Xie, X. S. *Science* **2003**, *302*, 262–266.
(24) Min, W.; English, B. P.; Luo, G.; Cherayil, B. J.; Kou, S. C.; Xie, X. S. *Acc. Chem. Res.* **2005**, *38*, 923–931.
(25) Gorris, H. H.; Rissin, D. M.; Walt, D. R. *Proc. Natl. Acad. Sci. U.S.A.* **2007**, *104*, 17680–17685.

Published on Web 03/05/2008

heterogeneity within a large number of turnover trajectories. These results are compared to bulk enzyme experiments.

The Michaelis–Menten equation is derived from bulk enzyme reactions where the velocities of millions of enzyme molecules are averaged. Using an impressive single molecule microscopy method, Xie and co-workers[16,24] have applied the Michaelis–Menten equation to single enzyme molecules. Averaging the waiting times between enzymatic turnovers over a long time trace for a single enzyme molecule demonstrated the viability of the Michaelis–Menten formalism at the single enzyme molecule level. Their results also shed light on the time fluctuation of the turnover rate, k_{cat}. While the experiments described here do not analyze the waiting times between successive catalytic turnovers, they track the velocities of large numbers of single molecules over long time periods. We have found that these velocities are highly distributed and long-lived, suggesting the presence of stable activity states on long time scales.

Materials and Methods

Enzyme Purification. β-Galactosidase from *Escherichia coli* was purchased from Sigma-Aldrich (Grade VIII) and purified using a Zorbax GF-450 size-exclusion HPLC column (Agilent) in PBS/$MgCl_2$ (2.7 mM KCl, 1.5 mM KH_2PO_4, 136 mM NaCl, 8.1 mM Na_2HPO_4, 1 mM $MgCl_2$, pH 7.3) (Supporting Figure 1). The identity of the purified enzyme was confirmed with MALDI (Applied Biosystems Voyager DE-PRO). The purified enzyme solution was mixed 1:1 in glycerol, aliquoted, and stored at −20 °C. The enzyme stock solution was diluted just prior to experimentation.

Bulk Enzyme Experiments. Bulk enzyme experiments were performed on an Infinite M200 microtiter plate reader (Tecan AG, Switzerland). Thirty-six picomolar final enzyme concentration (after dilution with substrate solution) was used at five RGP substrate concentrations (200, 100, 50, 25, 12.5 μM). The turnover rate at each substrate concentration was calculated by generating a resorufin standard curve.

Femtoliter Array Preparation. Bundled 4.5 μm optical fibers containing 50 000 individual fibers in a 2 mm bundle were purchased from Schott North America, Inc. The bundles were cut to length (typically 4–6 cm) and polished on both sides using a fiber polisher and a series of lapping films down to 0.3 μm grit. The cladding and core material of the optical array are both composed of silica but are doped with different materials. This way, the core can be selectively etched with hydrochloric acid. Using a solution of 0.025 M HCl with stirring, the core material etches at a rate of ~1.3 μm/min. The fibers were etched for 115 s, creating wells 2.5 μm deep, with a volume of 40 fL.

Experimental Setup and Vessel Sealing. The femtoliter array was blocked by incubating the fiber in PBS starting block blocking buffer (Pierce Biotechnology, Rockford, IL) for 30 min followed by rinsing with PBS buffer. Surface passivation is required for single molecule kinetic experiments using the microwell array. Experiments using unblocked arrays yielded irregular kinetic responses, which did not correlate with bulk enzyme kinetics (Supporting Figure 2). The blocked array was cleaned with a lint-free swab to remove blocking protein from the cladding material. The array was locked into the microscope stage using a custom-made fiber holder. The holder enables the fiber to withstand significant upward pressure without moving out of the focal plane. For vessel sealing, 0.01 in. non-reinforced gloss silicone sheeting material was used (Specialty Manufacturing Inc., Saginaw, MI). A small piece of silicone (~1 cm^2) was meticulously cleaned using soapy water followed by extensive rinsing with nanopure water (Millipore, Billerica, MA). The clean silicone sheeting readily adhered to a clean microscope slide, allowing solution deposition onto the gasket. A solution of RGP in PBS pH 7.4 buffer was placed onto the gasket followed by a 1:1 dilution and mixing with a low concentration solution of β-galactosidase in PBS pH 7.4 buffer. The solution was brought into contact with the etched wells of the array and allowed to sit for approximately 45 s to allow for the air trapped in the wells to be displaced (Supporting Movie 1). The gasket was brought into contact with the array to seal and isolate the wells and was followed by periodic image acquisition.

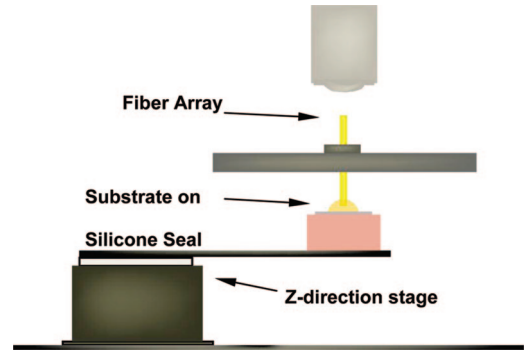

Figure 1. Single molecule assays using the microscope/mechanical platform system. A 2 mm hexagonally packed optical fiber bundle with 50 000 individual 40 fL reaction chambers on the distal surface is fastened to the microscope stage. A solution containing RGP and a low concentration of β-galactosidase (typically 1.0 pM) is deposited onto a cleaned silicone gasket. Using precision z-direction and tilt stages, the solution is brought into contact with the reaction chambers of the fiber array. After a short time (<1 min), the silicone gasket is moved into position, sealing off each femtoliter reaction chamber.

Optical Detection. A custom-built, epifluorescence imaging system acquired images. A short arc mercury lamp was used as the excitation source, while filter wheels controlled the wavelength's excitation and emission light that reached the sample and were collected by the CCD camera (Sensicam QE, Cooke Corporation, Romulus, MI), respectively. Images were taken every 15 s using an exposure time of 2000 ms. All images were analyzed using IPLab software (BD Biosciences, Rockville, MD). Sealing known concentrations of the fluorescent product resorufin into the vessels and constructing a calibration curve allowed single enzyme molecule velocities to be calculated.

Substrate Turnover Calculation. The photobleaching rate of the fluorescent product was determined by enclosing 10 μM resorufin in the microchambers and monitoring the fluorescence decrease every 15 s with an exposure time of 2000 ms over 50 min. An exponential fit of the data yielded a photobleaching rate, k_{ph}, of 0.0013 s^{-1} (Supporting Figure 3). The raw fluorescence intensities of the trajectories (Figure 2) were multiplied by the calibration factor and background corrected. The substrate turnover was calculated using the equation $S(t) = F'(t) + k_{ph} \times F(t)$, where $S(t)$ is the substrate turnover of a single enzyme molecule in the microchamber, $F(t)$ is the fluorescence intensity as a function of time, $F'(t)$ is its time derivative, and k_{ph} is the photobleaching rate. A median filter of length 11 was used for Figure 3C to smooth $F'(t)$.

Results and Discussion

In this work, we employed β-galactosidase from *Escherichia coli*, a 465 kDa enzyme that contains four identical catalytic sites and is only active as a tetramer.[26] β-Galactosidase catalyzes the hydrolysis of β-galactosides. The commercial enzyme preparation was purified by size-exclusion HPLC to ensure a homogeneous enzyme population and to remove enzyme aggregates (Supporting Figure 1). For the β-galactosidase assays performed here, the nonfluorescent substrate resorufin-β-D-galactopyranoside (RGP) was used. By monitoring the catalytic

(26) Marchesi, S. L.; Steers, E., Jr.; Shifrin, S. *Biochim. Biophys. Acta* **1969**, *181*, 20–34.

Figure 2. Seal-and-release experiments. An enzyme solution was sealed into the array of femtoliter reaction chambers until a significant amount of fluorescent product accumulated in the reaction chambers. The seal was repeatedly released and sealed, allowing for significant product accumulation after each sealing step.

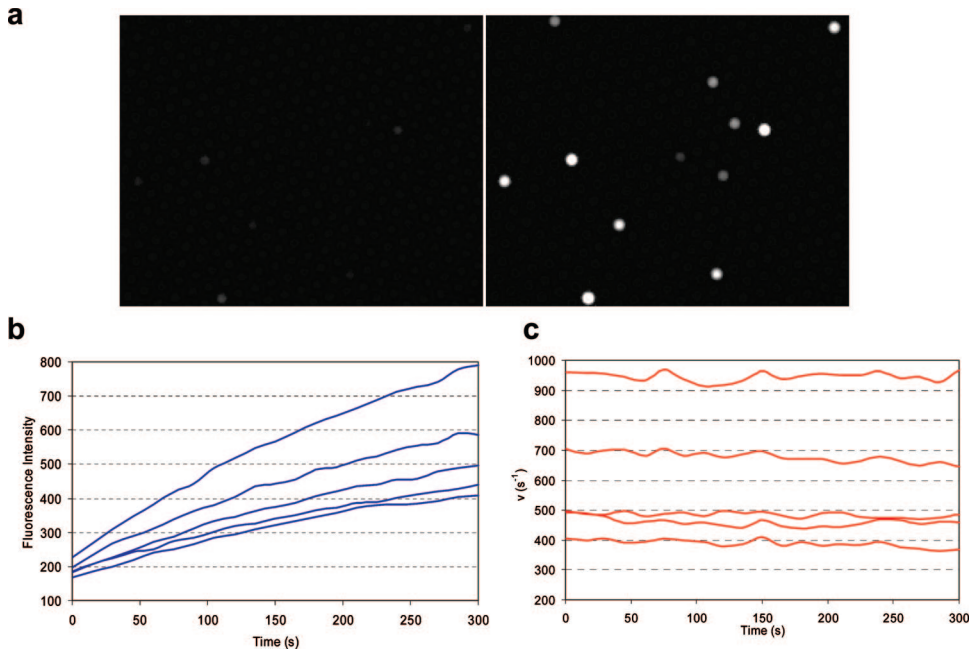

Figure 3. Single molecule catalytic rates show wide static variation. (a) Images of a small section of the array of femtoliter reaction chambers at the start of a single molecule experiment (left) and the same portion of the array after 10 min elapsed showing different levels of product (right). (b) Time traces of product formation of five representative enzyme molecules from a single experiment monitoring over 190 individual enzyme molecules using 100 μM RGP solution. (c) Time derivative of the traces in (b) plotted as velocity (s^{-1}), using an 11-point median filter and photobleaching correction factor. Steady, highly distributed rates of product formation suggest the presence of stable β-galactosidase conformers.

hydrolysis of RGP to highly fluorescent resorufin, kinetic information from large populations of single enzyme molecules was collected at various substrate concentrations. We have implemented a high-density array of 50 000 40 fL reaction chambers[27,28] on the distal face of an etched optical fiber bundle to enclose single β-galactosidase molecules with various RGP concentrations. The probability $P(x)$ that exactly x enzyme molecules are enclosed in a certain reaction chamber is given by the Poisson distribution, which applies to a rare event occurring given a large number of trials:

$$P_{\mu}(x) = \frac{e^{-\mu}\mu^{x}}{x!} \qquad (1)$$

where μ is the mean number of enzymes per microchamber. If a ratio of one enzyme molecule to 20 microchambers is used, more than 95% of the microchambers are empty and 4.8% contain a single enzyme molecule. Using an enzyme concentration of 1.8 pM in combination with an array of 40 fL reaction chambers yields a 1:20 ratio.[28] The reaction chambers were sealed with a silicone gasket on the array face to confine individual enzyme molecules and their catalytic products (Figure 1). A custom-built epifluorescence microscope system was used to simultaneously monitor the substrate turnover of a large population of single enzyme molecules in the reaction chambers.

In order to ensure that the individual enzyme molecules do not stick to the reaction chamber surface, seal-and-release experiments were conducted (Figure 2).[12] By sequentially sealing and releasing solution from the femtoliter reaction chambers, single enzyme molecule activity was observed at different, random positions. This result shows that the enzymes are not surface-bound and are free in solution during the assay, suggesting that the femtoliter reaction chambers can be used to monitor the kinetics of single enzyme molecules without influencing their activity.

Single molecule experiments were run for 2 min with measurements taken every 15 s. By measuring the product of thousands of single enzyme turnover events, any heterogeneity in the occupation of the enzyme's four active sites is eliminated and the turnover rates from molecule to molecule can be compared. Varying rates of activity from molecule to molecule were evident through visual inspection (Figure 3a). Taking the

(27) Rissin, D. M.; Walt, D. R. *J. Am. Chem. Soc.* **2006**, *128*, 6286–6287.
(28) Rissin, D. M.; Walt, D. R. *Nano Lett.* **2006**, *6*, 520–523.

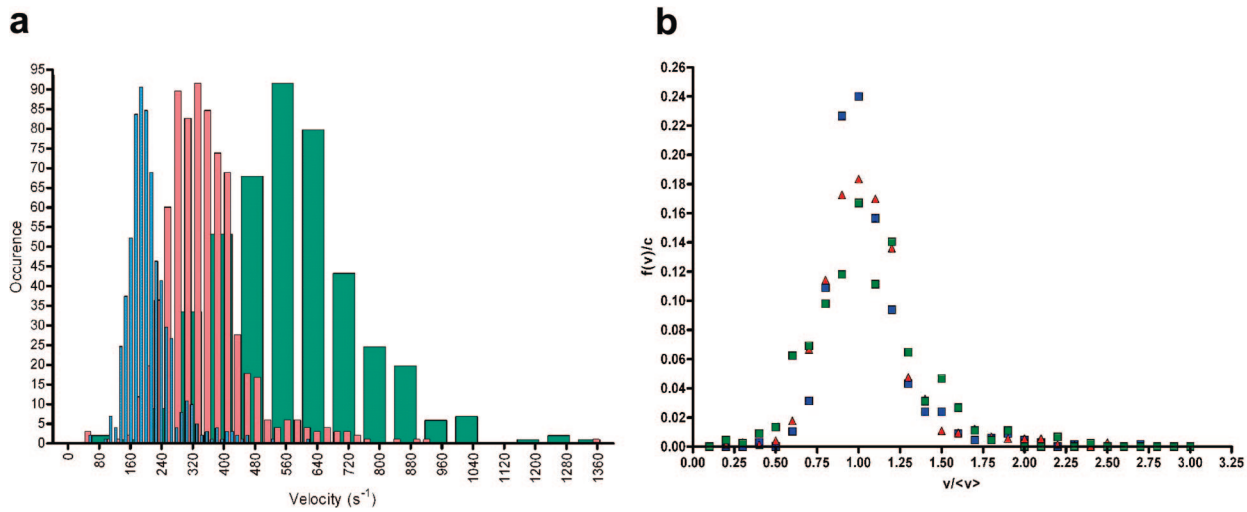

Figure 4. Single molecule turnover distribution histograms. (a) The normalized velocity occurrences at substrate concentrations of 25 μM (blue), 50 μM (red), and 150 μM (green) are shown. The 25, 50, and 150 μM histograms were normalized using 12.5, 25, and 75 s^{-1} bin widths, respectively. Each histogram plots hundreds of single molecule turnover rates, combined from multiple experiments. (b) The normalized velocity frequency distribution of 25 μM (blue), 50 μM (red), and 150 μM (green) substrate concentrations. Similar coefficients of variation suggest that the distribution is isolated to k_{cat}.

time derivative of the fluorescence intensities yields the substrate turnover rate (v), which is adjusted for photobleaching by correcting for the exponential rate of bleaching of the fluorescent product, resorufin (Figure 3b,c).

To accurately calculate the substrate turnover rate, it is important that the substrate concentration remains constant over time. At low RGP concentrations, the enzyme activity leads to the highest percentage of substrate depletion. The lowest RGP concentration employed was 25 μM, where each 40 fL reaction chamber contained approximately 602 000 substrate molecules. The average substrate turnover rate at 25 μM was 233 s^{-1}, resulting in an average depletion of less than 5% of the substrate after the 2 min experiment. Accordingly, while the reaction chamber volume is small enough to segregate single enzyme molecules and accumulate a readily detectable product concentration, it is also large enough to hold a sufficient number of substrate molecules to ignore substrate depletion effects.

Experiments were conducted with 25, 50, 100, 150, and 200 μM substrate concentrations, with each experiment tracking the activity of approximately 200 enzyme molecules. The average velocity of the single enzyme molecules exhibited a hyperbolic dependence on the substrate concentrations according to the Michaelis–Menten equation. Averaged single molecule and bulk K_M values were in agreement: the average single molecule $K_M = 76 \pm 12$ μM and bulk $K_M = 117 \pm 23$ μM. In addition, the single molecule experiments provided an averaged maximal velocity of 916 ± 58 s^{-1} compared with 888 ± 87 s^{-1} for the bulk experiments.

While the average single molecule turnover velocities are in agreement with bulk enzyme experiments, the distribution in activity from molecule to molecule at a given substrate concentration was surprisingly large. The wide distribution of activities shown in the histograms (Figure 4a) confirms the presence of heterogeneity within enzyme populations. The histograms relate the velocity distribution of single enzyme molecules to substrate concentration and confirm results from other laboratories that observed large variations of enzyme activities within a population.[1–4,29,30]

Conventionally, the velocity of an enzymatic bulk reaction is defined as $d[P]/dt = k_{cat}[ES]$. Under steady state conditions and if $[S] >> [E]$, $[ES]$ can be expressed by $[E]_T[S]/(K_M + [S])$. In a single enzyme molecule experiment, however, it is meaningless to define a concentration $[ES]$, as a single enzyme molecule is either in a state in which it has bound a substrate molecule or it is free. A single molecule Michaelis–Menten equation can be obtained if $[ES]$ is replaced by the probability of finding the enzyme in the enzyme–substrate complex.[24] As our single enzyme molecule trajectories represent thousands of substrate turnovers at each measurement, we can define $d[P]/dt = k_{cat}\rho_{ES}$, where ρ_{ES} is the probability that the enzyme will be in the ES form. In analogy to the Michaelis–Menten equation, but without the restrictive condition $[S] >> [E]$, the probability of finding the enzyme molecule bound in an enzyme–substrate complex is given by $\rho_{ES} = ([S]/K_M + [S])$. Thus, one can obtain a single molecule Michaelis–Menten equation, where v_i indicates the velocity of an individual enzyme molecule:

$$v_i = k_{cat}\left(\frac{[S]}{K_M + [S]}\right) \quad (2)$$

One source for variability in v_i is the probability of finding a single enzyme molecule in the enzyme–substrate complex ρ_{ES}; ρ_{ES} is dependent on K_M, but with increasing $[S]$, K_M has less influence on the enzyme reaction; any variability in the enzyme–substrate complex formation should decrease at higher $[S]$. If, on the other hand, differences in k_{cat} are the source of heterogeneity in v_i, then the variability should be independent of $[S]$ and the velocity ***distribution*** should be identical for all $[S]$. Figure 4a shows a wide velocity distribution of the individual β-galactosidase molecules. The frequency distributions of the normalized data ($v_i/<v>$) superimpose at substrate concentrations of 25, 50, and 150 μM and have the same coefficient of variation ($30 \pm 1\%$) (Figure 4b). Therefore, the velocity distribution can be assumed to be a universal function

(29) Craig, D. B.; Hall, T.; Goltz, D. M. *BioMetals* **2000**, *13*, 223–229.

(30) Shoemaker, G. K.; Juers, D. H.; Coombs, J. M. L.; Matthews, B. W.; Craig, D. B. *Biochemistry* **2003**, *42*, 1707–1710.

of [*S*]. This result suggests variability in k_{cat} is responsible for the wide distribution of v_i.

Conclusion

In these single molecule experiments, the distribution of activities is significant and is a product of numerous stable activity states of β-galactosidase. Analyzing normalized velocity distributions across various substrate concentrations provided additional information. We have found the normalized distributions to be identical at all substrate concentrations, suggesting that variability in k_{cat} is responsible for the distributed activity states of β-galactosidase. Our result supports previous findings that have shown dynamic disorder to be isolated to the turnover rate (k_{cat}).[16] We speculate that rapidly changing conformations on short time scales[16,24] are a subset of an enzyme molecule's unique and predominantly stable primary activity state. These results provide additional insight into the underlying contributors to the distribution of activities within a population of ostensibly identical enzyme molecules. The implications of this activity distribution on metabolic pathways are most likely significant but remain to be determined.

Acknowledgment. We thank Subrahmanian Tarakkad Krishnaji from the Kumar group in Tufts Chemistry Department for his help with the size-exclusion chromatography. We thank Professor X. Sunney Xie and graduate students Brian English and Wei Min from Harvard University for their critical review and helpful suggestions.

Note Added in Proof. D.R.W. is a Professor at Tufts University and is the founder and a director of Quanterix, a company that has licensed technology from Tufts University that is pursuing applications of the single molecule detection method described in this paper. D.M.R. was a graduate student at Tufts University when he completed the work described in the paper and is now employed by Quanterix.

Supporting Information Available: Two figures and one movie supporting the Materials and Methods section. This material is available free of charge via the Internet at http://pubs.acs.org.

JA711414F